I&EC research
Industrial & Engineering Chemistry Research

pubs.acs.org/IECR

Article

Pt-Catchment Using Pd/Au Alloys: Effect of Enhanced Diffusion

Asbjørn Slagtern Fjellvåg,* David Waller, Thomas By, and Anja Olafsen Sjåstad*

Cite This: *Ind. Eng. Chem. Res.* 2023, 62, 2478−2493

Read Online

ACCESS | Metrics & More | Article Recommendations | Supporting Information

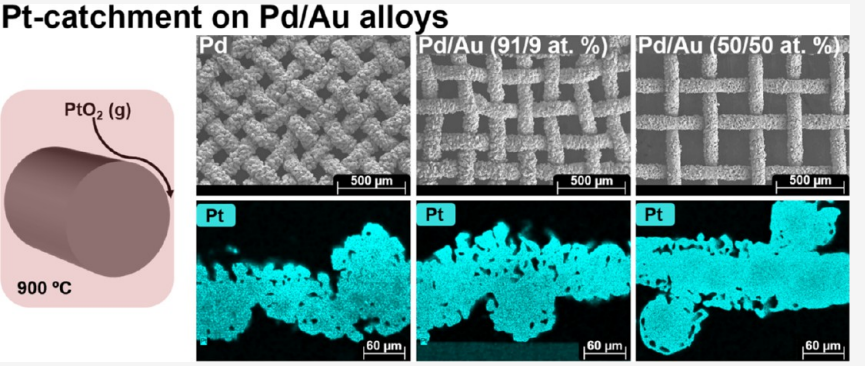

ABSTRACT: We have studied a series of Pd/Au alloys as Pt-catchment materials, both in lab-scale experiments and in an industrial ammonia oxidation plant. Our focus has been on how bulk Pt diffusion affects grain reconstruction in Pd/Au alloys (91/9 and 50/50 at. %) during Pt-catchment, performed by studying both polycrystalline (as produced) and quasi-monocrystalline (preannealed in vacuum) wires. The grain reconstruction is reduced when alloying Pd with Au, and it is almost absent for Pd/Au (50/50 at. %). For all Pd-containing samples with a quasi-monocrystalline grain structure, the restructuring is limited in short (<20 days) laboratory experiments but present in the 5 month industrial experiment. Notably, the Pd/Au (50/50 at. %) alloy shows a low degree of restructuring in all experiments but a reduced Pt-catchment in the industrial experiment. The mechanism for grain reconstruction of Pd/Au alloys is discussed, along with the role of the Kirkendall effect and the internal porosity on wire restructuring.

1. INTRODUCTION

In the industrial production of synthetic nitrogen-based fertilizer, one of the key reaction steps is the oxidation of ammonia to nitric oxide (NO) over a Pt/Rh (83/17−91/9 at. %) catalytic gauze, performed at 800−950 °C and 1−12 bar.[1] The ammonia oxidation reaction is highly exothermic, and the generated heat causes local hotspots on the catalyst surface, giving rise to Pt and Rh evaporation in the form of volatile oxide molecules in a chemical vapor transport process. Parts of the evaporated noble metal oxides condense and form cauliflowers on the catalyst surface by a vapor condensation mechanism, but a significant amount is permanently lost from the catalyst, mainly Pt.[2] To reduce the Pt-loss during operation, a Pd/Ni-catchment gauze (woven net) is installed below the Pt/Rh catalyst to capture the lost Pt. Unfortunately, the Pd/Ni wires are victim to severe structural reconstruction and pore formation during operation, causing the Pd/Ni net to convert into a porous plate-like structure. The poor flow conditions through the reconstructed Pd/Ni net causes a significant pressure drop to build up, limiting the number of Pd/Ni gauzes that can be installed simultaneously. Additionally, the Pd/Ni-catchment unit suffers from severe Pd loss, which is barely compensated for by the quantity of Pt it can capture (with metal prices of March 2022).[3,4] Over the last few years, the metal price of Pd has continuously increased compared to Pt, causing a large Pd loss to be detrimental to the future use of the Pd/Ni catchment system (Figure S11). The lack of good Pt-catchment solutions is continuously a significant expense in the production of nitric acid.

The original Pt-catchment system, Pd/Au (88/12 at. %), was invented by Holzmann and the Degussa company in 1968.[5] He showed that the entire $Pd_{1-x}Au_x$ system could capture Pt, but the Au-rich alloys performed poorly as Pt-catchment systems compared to Pd. The only exception was Au, which was approximately as good as Pd/Au (88/12 at. %). However, the mechanical properties of both Au and Pd caused the Pd/Au (88/12 at. %) alloy to be selected as the industrial Pt-catchment system. Since then, several studies have been performed on both Pd/Au and the more recent Pd/M (M = Co, Ni, Cu) systems.[3,4,6−18] The latest studies on Pd and Pd/Ni (91/9 at. %) wires showed that the pore formation observed during

Received: August 9, 2022
Revised: January 23, 2023
Accepted: January 25, 2023
Published: February 3, 2023

industrial operation originates from two different phenomena: (1) thermal etching related to extreme gas/temperature conditions, giving a *rounded* crystallite shape and (2) grain reconstruction during Pt-catchment giving an *edged* crystallite shape.[3] The grain reconstruction process (2), is described as a corrosion process caused by gas-phase platination.[4] Rapid grain boundary (GB) diffusion of Pt (into) and Pd (outward) of the Pd and Pd/Ni wires causes a complete restructuring of the entire grain structure, and clear faceted (edged) crystals are formed. Interestingly, quasi-monocrystalline samples did not restructure to the same extent. They also captured less Pt[4] due to a gas-surface equilibrium between gaseous PtO_2 and the high concentration of solid Pt on the surface. The Kirkendall effect, in both bulk and the GBs,[19−26] is considered the main suspect for causing the wire reconstruction, in the sense that Kirkendall voids (internal voids) are formed by agglomeration of vacancies inside the wire. However, this mechanism has not yet been proven, even though Pd is reported as the faster diffusing species in the Pd−Pt system.[27]

It seems like the ratio of the GB and bulk diffusion rates is a valid descriptor for predicting the degree of grain reconstruction.[4] Hence, an improved bulk diffusion may reduce the grain reconstruction during Pt-catchment. In this experimental work, we have therefore returned to the very same Pd/Au system as explored by Holzmann in 1968[5] with the purpose to understand the true Pt-catchment potential of this system. The alloying of the Pd nets with Au should significantly enhance the diffusion properties of the materials due to the substantially lower melting point of Au (1063 °C) compared to Pd (1552 °C) and the higher reported self-diffusion coefficient[28] (Table S4). Additionally, Pd, Pt, and Au show good solid solubility with each other.[28,29] Despite several old investigations of the Pd−Au and Pd−Au−Pt systems,[30−34] there is still a lack of a reliable source of diffusion data for the alloys in the two systems at relevant temperatures. The diffusion coefficients used in this work are only estimates (Table S4). However, the reported Pt-diffusion in Au is 3−4 orders of magnitude higher than in Pd. Our estimated diffusion coefficients for Pt in Pd/Au is slightly higher than the reported interdiffusion coefficients in Pd/Au,[35] which correlate well with the fact that Pt diffusion in Au is 1−2 orders of magnitude lower than the self-diffusion in Au.[28,29] In this work, Pd, Au, and two different Pd/Au alloys (91/9 and 50/50 at. %) are evaluated as potential Pt-catchment materials, chosen to cover an appropriate range of Pd/Au compositions and see the contrast between 9 at. % Au or Ni in the Pd alloy. The materials are tested both in the laboratory and in a 5 month industrial experiment, including Pd/Ni (91/9 at. %) in the industrial experiment. Our focus is on Pt-catchment abilities, diffusion, and the degree of grain reconstruction.

2. MATERIALS AND METHODS

Noble metal wires and nets (diameter of 76 μm) (100 μm for Au) with compositions Pd, Pd/Au (85/15 wt. %, 91/9 at. %), Pd/Au (35/65 wt. %, 50/50 at. %), Au, and Pd/Ni (95/5 wt. %, 91/9 at. %) were produced by K. A. Rasmussen with a purity >99.9%. Samples used in the laboratory experiments and industrial plant experiments originate from the same source of polycrystalline wires, with a grain size of 5−20 μm. For several of the experiments, the polycrystalline samples were transformed into quasi-monocrystalline samples by preannealing for 7 days at 1100 °C (900 °C for Au) in a double-evacuated quartz ampoule, prior to use. The grain sizes of the quasi-monocrystalline wires are confirmed to be in the range of 50−200 μm.

For the laboratory-scale furnace experiments, samples were heat-treated in a six-zone furnace operated at 900 °C (ambient pressure) using a quartz tube with an inner diameter of 6 mm and a 1 L/min flow of air.[3] The air was dried with a freeze drier, an absorption drier, and a H_2O purifier. A Pt net (∼350 mg) was positioned upstream of the catchment samples, at 1000 °C, to produce PtO_2 vapor of $4−5 \times 10^{-8}$ bar. Prior to the Pt-catchment experiments, the catchment wires (∼20 cm) were twinned to a spiral and placed in the quartz tube. The mass of the entire wire was determined before and after the experiments. The front part of the spiral (∼2 cm) was investigated with scanning electron microscopy (SEM)/EDX, and the next part (∼5 cm) was sent for inductively coupled plasma optical emission spectroscopy (ICP−OES)/MS analysis (see below). The experiments were run for 5, 10, and 20 days. The data after 10 days are presented in the Supporting Information. The tail of the 20 days Au wire was run for another 20 days to achieve 40 days, but then the sample had not experienced a maximal PtO_2 exposure during the first 20 days of the experiment (presented in the Supporting Information). For the quasi-monocrystalline (preannealed) samples, the experiment was run for 20 days and the two Pd/Au alloys were treated in the form of nets.

Samples treated in the industrial plant of Yara International (Herøya, Norway) were carefully prepared to minimize uncertainties in the mass change and avoid interactions with physical objects/particles in the gas stream (e.g., oxide particles) (Figure 1). Net samples of all alloys were cut into a unique shape

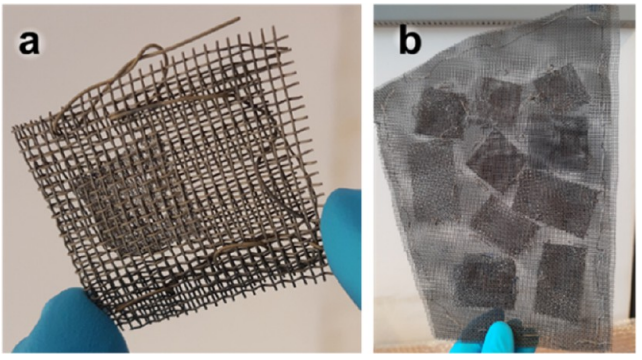

Figure 1. Photos showing how the industrial samples were prepared (taken after the experiment). (a) One sample sewed into the megapyr sandwich and (b) the entire sample pack after being sewed together.

in order to distinguish the samples from each other after the experiment. The samples (∼3−4 cm^2) were placed in a megapyr net ($Cr_{0.20}Al_{0.5}Fe_{0.75}$) folded around the samples (as a sandwich), which was then sewn together with a megapyr wire. The samples were weighed three times; prior to sample preparations, with the megapyr net, and with the megapyr net after sewing it together. The process was finalized by placing all samples between two large pieces of a megapyr net, which were sewn together. Inside the sandwich, a reference megapyr net was also placed along with the samples to know the weight change of the megapyr alloy during the experiment (due to oxidation). The prepared sample sandwich was located on top of the N_2O decomposition catalyst and below (downstream) the ammonia oxidation catalyst (Pt/Rh) and the Pt-catchment gauzes (Pd/Ni). The reactor was operated for 5 months with a temperature of 890 °C and 5 bar, and the gas mixture contained 10.2 vol. % NH_3 in compressed air before hitting the ammonia oxidation catalyst. The gas mixture at the sample location was

https://doi.org/10.1021/acs.iecr.2c02852
Ind. Eng. Chem. Res. 2023, 62, 2478−2493

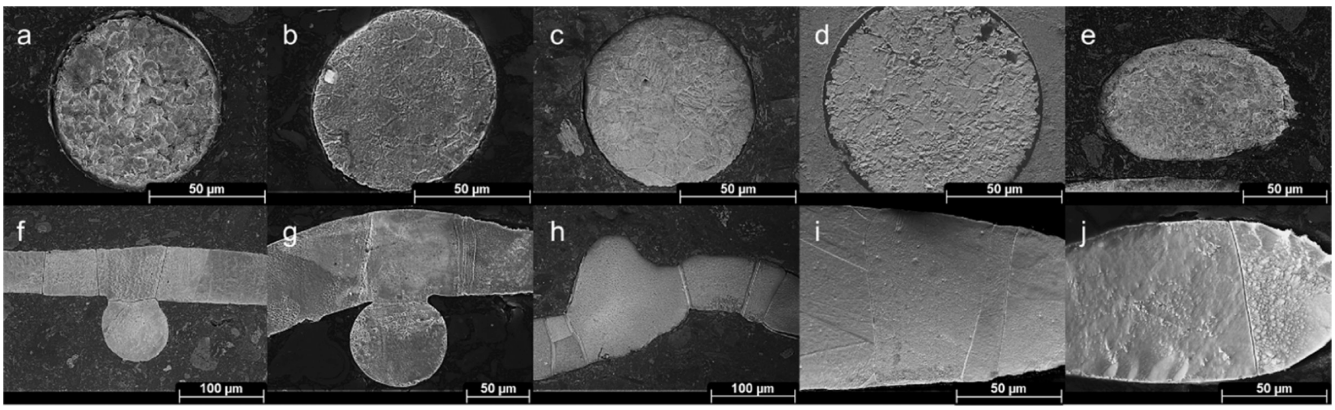

Figure 2. SEM images of etched wire cross sections. The top row (a–e) shows the grain structure of the polycrystalline samples: (a) Pd, (b) Pd/Au (91/9 at. %), (c) Pd/Au (50/50 at. %), (d) Au, and (e) Pd/Ni (91/9 at. %). The bottom row (f–j) shows the grain structure of the quasi-monocrystalline samples: (f) Pd, (g) Pd/Au (91/9 at. %), (h) Pd/Au (50/50 at. %), (i) Au, and (j) Pd/Ni (91/9 at. %).

Table 1. Pt Concentration in the Different Polycrystalline Samples Obtained from Mass Changes, Assuming All Mass Gain Is Caused by Pt-Catchment (Left) and the Elemental Content (at. %) of Pd, Au, and Pt Obtained from ICP–OES Analysis (Right) after Pt-Catchment Experiments at 900 °C in Air[a]

	from mass change		ICP–OES(after 20 days)			
polycrystalline	Pt (5 days)[at. %]	Pt (20 days)[at. %]	Pd [at. %]	Au [at. %]	Pt [at. %]	Pd/(Pd + Au)[at. %]
Pd/Au(91/9 at.%)	4.9	8.3	81.3	8.8	9.9	90.3
Pd/Au(50/50 at. %)	4.0	8.6	45.3	44.6	10.1	50.4
Au	3.6	4.7		89.9	10.1	
Pd (10 days)*			79.9		20.1	

[a]ICP–OES data for Pd tested for Pt-catchment for 10 days is included for comparison (*).[4]

approximately 9 vol. % NO, 15 vol. % H_2O, 6 vol. % O_2, 2000 ppm N_2O, and the rest N_2. The samples were assumed to react homogeneously with the gas mixture over the entire net, and approximately, 1 cm^2 of each net was sent for ICP–OES/MS analysis, while the rest was analyzed with SEM/EDX. SEM/EDX analysis was performed on both the gas in-flow side (*up*) and the gas out-flow side (*down*) of the samples. The polycrystalline Pd/Ni sample was treated in a different net package and was different in size (90 μm). This may affect the comparability of these samples with the other samples.

SEM–EDX was performed with a Hitachi Ultra High Resolution 8230 field-emission SEM. Images were obtained by collecting the low-energy electrons produced by the electron beam with an acceleration voltage of 1 kV. EDX analysis (mapping and point quantification) was performed using an acceleration voltage of 30 kV. For surface analysis, the samples were mounted with a carbon tape on a copper plate. For cross-sectional imaging, the samples were cast in a conducting resin containing carbon fiber (PolyFast, Struers, Denmark) before grinding and polishing (1 μm diamond finish).

To map the grain structure of the samples, the samples were cast in a conducting resin (Polyfast, Struers), grinded and polished, and then etched in order to see the grain structure. Etching of wire cross sections was performed using mixtures of HCl and HNO_3 (from 50/50 to 75/25 mol % mixtures). Depending on the samples, they were immersed in the acid from 30 s to 6 min. A variating result is obtained each time due to the inconsistency of the etching, so several attempts were performed for each sample, with surface polishing in between each etching.

ICP–OES/MS analyses were carried out by Mikrolab Kolbe (Fraunhofer Institute in Oberhausen, Germany). Acid digestion was used to dissolve the samples, with a special high temperature and pressure digestion approach for rhodium. The samples were measured with an ICP–OES Spectro Arcos from Spectro and checked with an AAS Contra 800 from AnalytikJena. The estimated error of the measurement is 0.015% absolute for Ni, 0.025% absolute for Pt in samples with more than 15% Pt, 0.04% absolute for Pt in samples with less than 15% Pt, and 0.055% absolute for Pd.

MATLAB[36] was used for diffusion simulations, relying on the diffusion model developed by Fjellvåg et al.[4] using estimated diffusion coefficients for the two mixed Pd/Au compositions (Table S4).

3. RESULTS

3.1. Analysis of Grain Structure Prior to Experiments. Pd/Au alloys with two different grain structures were used in the current Pt-catchment experiments. SEM images of the etched cross sections of both polycrystalline and quasi-monocrystalline wires are presented in Figure 2. All polycrystalline samples have a grain size of ~5–20 μm (Figure 2a–e), while the quasi-monocrystalline samples have a grain size of ~30–200 μm (Figure 2f–j). It is evident from the images in Figure 2 that the polycrystalline samples generally have a significantly smaller grain size than the quasi-monocrystalline wires.

3.2. Laboratory Experiments with Pd/Au Alloys for Pt-Catchment. *3.2.1. Polycrystalline (as-Produced) Pd/Au Alloys.* Two different Pd/Au compositions (91/9 and 50/50 at. %) and Au were tested as potential Pt-catchment materials in a gas stream of air with PtO_2 (g) for 5 and 20 days. Pt content calculated from mass changes (5 and 20 days) and ICP–OES measurements (20 days) are reported in Table 1. For all samples, there is an increase in the Pt content with time, as expected during Pt-catchment. The Pt content is very similar for all

https://doi.org/10.1021/acs.iecr.2c02852
Ind. Eng. Chem. Res. 2023, 62, 2478–2493

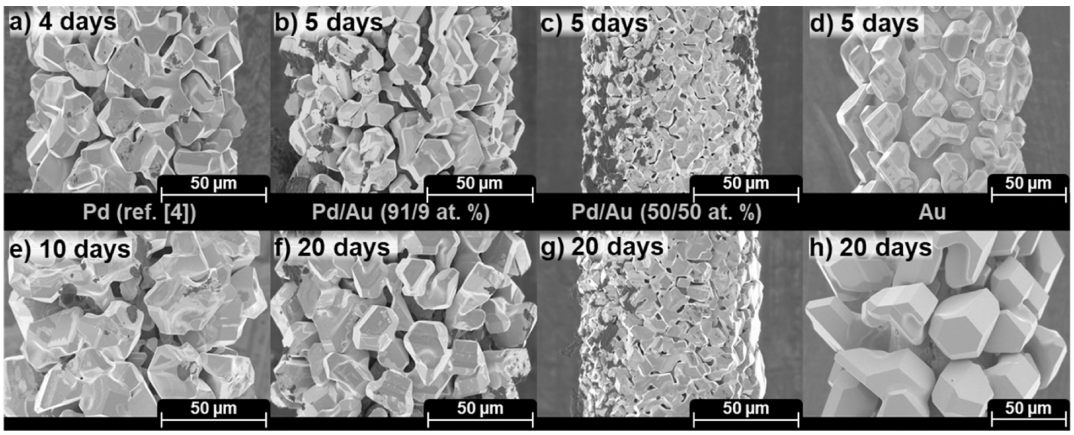

Figure 3. SEM images showing the development of the surface of the polycrystalline Pd/Au samples during Pt-catchment at 900 °C in air. (a) Pd after 4 days (from Fjellvåg et al.[4]), (b) Pd/Au (91/9 at. %) after 5 days, (c) Pd/Au (50/50 at. %) after 5 days, (d) Au after 5 days, (e) Pd after 10 days (from Fjellvåg et al.[4]), (f) Pd/Au (91/9 at. %) after 20 days, (g) Pd/Au (50/50 at. %) after 20 days, and (h) Au after 20 days. SEM images after 10 days (and 40 days for Au) are shown in Figure S1.

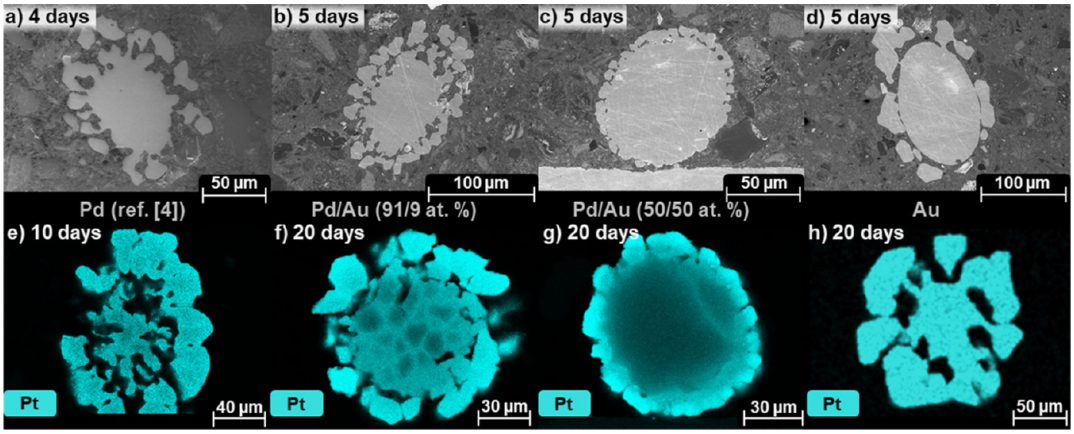

Figure 4. SEM images (after 5 days) and EDX maps (after 20 days) of the wire cross section for the polycrystalline Pd/Au samples after Pt-catchment experiments at 900 °C in air. (a) Pd after 4 days (from Fjellvåg et al.[4]), (b) Pd/Au (91/9 at. %) after 5 days, (c) Pd/Au (50/50 at. %) after 5 days, (d) Au after 5 days, (e) Pd after 10 days (from Fjellvåg et al.[4]), (f) Pd/Au (91/9 at. %) after 20 days, (g) Pd/Au (50/50 at. %) after 20 days, and (h) Au after 20 days.

samples, reaching ∼10 at. % Pt after 20 days, according to the ICP−OES analysis. However, compared to Pd treated for 10 days by Fjellvåg et al.,[4] the Pt content (at. %) is lower in the Pd/Au samples. Notably, the observed mass change underestimates the Pt content relative to the ICP−OES measurements for all samples. The Au sample shows the most severe underestimation of the Pt content from the mass change analysis. It is likely that the general handling of the sample may result in physical material loss as the surface crystals in the Au sample were very loosely attached (Figure S1). For the two Pd/Au samples, we find it more likely that the underestimation of the Pt content from the mass change analysis is caused by the fact that the pieces sent for ICP−OES analysis were collected from the front half of the wire, which may contain more Pt than the entire sample on average. A third option is the possibility of a volatile loss of Pd or Au during the experiment. However, previous reports do not indicate a significant mass loss of Pd or Au in air,[3,5,37] and we find this option unlikely. Because of these results, we generally trust ICP−OES data more than the mass change analyses.

During Pt-catchment, it has been well documented that grain reconstruction occurs rapidly for the Pd-based wire[4] (Figure 3a,e). For all samples, several surface crystallites are formed and cover the entire surface (Figure 3). The surface crystallites vary in size depending on the wire composition, and the degree of surface restructuring varies depending on the wire composition. These are best compared by looking at the wire swelling (Figure 3) or the porosity seen from the cross section (Figure 4). For the Pd/Au (91/9 at. %) alloy, severe surface reconstruction occurs (Figure 3b,f), similar to Pd (Figure 3a,e). However, for the Pd/Au (50/50 at. %) alloy, the reconstruction occurs to a much lesser extent (Figure 3c,g). There is also a clear difference in the development with time; the Pd/Au (91/9 at. %) alloy shows a large increase in wire radius during the experiments, while the Pd/Au (50/50 at. %) alloy does not swell significantly during the experiment. Heat treatment in air at 900 °C without PtO_2 (g) present causes, as expected, no reconstruction of the Pd/Au samples (Figure S2).

The development of the Au wire is quite different. Large crystallites are already formed on the surface after 5 days, and they have developed significantly in size after 20 days (Figure 3d,h). The shape, size, and distribution of the surface crystals on the Au sample differs from the other compositions (Figure 3). The crystallites formed on the Au wire are very large, up to 40 μm after 20 days of Pt-catchment. Furthermore, they are loosely attached to the remaining core of the Au wire and fall off easily

https://doi.org/10.1021/acs.iecr.2c02852
Ind. Eng. Chem. Res. 2023, 62, 2478−2493

Table 2. Elemental Concentrations of Pd, Au, and Pt (at. %) Extracted from EDX Analysis of Polycrystalline Samples after 5 and 20 Days of Pt-Catchment Experiments at 900 °C in Air

	Pd/Au(91/9 at. %)		Pd/Au(50/50 at. %)		Au
polycrystalline, 5 days	Pt [at. %]	Pd/(Pd + Au)[at. %]	Pt [at. %]	Pd/(Pd + Au)[at. %]	Pt [at. %]
surface	50	93	50	56	11
cross section, surface crystal	18	95	38	68	9
cross section, edge of wire core	8	91	16	52	7
cross section, center of wire core	1	90	2	47	6
	Pd/Au(91/9 at. %)		Pd/Au(50/50 at. %)		Au
polycrystalline, 20 days	Pt [at. %]	Pd/(Pd + Au)[at. %]	Pt [at. %]	Pd/(Pd + Au)[at. %]	Pt [at. %]
surface	29	96	34	61	12
cross section, surface crystal	22	94	30	58	10
cross section, edge of wire core	15	91	16	49	10
cross section, center of wire core	8/10[a]	88	3	43	10

[a]Dark/bright regions in the EDX map in Figure 4.

Table 3. Elemental Concentrations of Pd, Au, and Pt (at. %) Determined from Mass Change Analyses (Assuming All Mass Gain is Caused by Pt-Catchment) and ICP−OES for Quasi-monocrystalline Pd/Au Samples Tested as Pt-Catchment Materials for 20 days at 900 °C in Air[a]

	mass change	ICP−OES(after 20 days)			
quasi-monocrystalline	Pt content after 20 days[at. %]	Pd [at. %]	Au [at. %]	Pt [at. %]	Pd/(Pd + Au)[at. %]
Pd/Au (91/9 at. %)	3.2	84.5	8.4	7.1	90.9
Pd/Au (50/50 at. %)	4.3	44.2	46.0	9.7	49.0
Au	6.7	0.0	90.4	9.6	
Pd (10 days)*	2.3				

[a]ICP−OES data for Pd tested for Pt-catchment for 10 days is included for comparison (*).[4]

during handling. This may explain why the Pt content of the Au wire is strongly underestimated from the mass change analysis (Table 1).

By viewing the wire cross sections of the exposed samples, we can see how deep into the wires the grain reconstruction process has occurred (Figure 4). According to Fjellvåg et al.,[4] a Pd wire (76 μm diameter) is expected to be completely reconstructed after 10 days. However, for the Pd/Au samples (76 μm diameter), the wire core remains intact after 20 days. The remaining wire core is ∼40 μm for Pd/Au (91/9 at. %) and ∼70 μm for Pd/Au (50/50 at. %). This indicates that during an extended period of Pt-catchment, the morphology of the Pd/Au (50/50 at. %) wire is stable. The Au wire keeps a remaining wire core of ∼70 μm (starting diameter 100 μm). We can also see from several SEM images (Figures 4d,h; 3d,h) that the surface crystallites are barely attached to the surface of the Au wire (Figure S1c,d,g,h) compared to the Pd/Au samples (Figure S1a,b,e,f).

The differences in the Pd/Au composition affect not only the morphology but also the ability to capture Pt. Even though the total Pt content is similar for the three Au-containing samples (Table 1), the EDX maps in Figure 4f−h show significant variations in the Pt distribution. For the two Pd/Au alloys, the Pt concentration is highest in the crystallites on the surface and is reduced toward the wire core (Table 2). Pd/Au (91/9 at. %) also shows a GB-like pattern in the EDX cross-section map (Figure 4f), where the bright/dark spots correlate with high/low Pt concentrations. The Pd/Au (91/9 at. %) sample also has a much higher Pt concentration in the wire core compared to Pd/Au (50/50 at. %), which is probably related to a more prominent GB diffusion in Pd/Au (91/9 at. %) and the fact that this sample has a smaller wire core (shorter diffusion distances).

For Au, the Pt distribution is completely homogeneous with ∼10 at. % Pt throughout the entire wire after 20 days (Figure 4h) (Table 2). However, Au also has a Pt concentration gradient after 5 days, at which point the wire core only contains ∼6 at. % Pt. This illustrates nicely the effect of rapid bulk diffusion in Au, especially when considering that the pure Au wire was 100 μm when the experiment started, not 76 μm like the two Pd/Au wires.

The grain structure of Pd/Au (91/9 at. %) is much more visible than Pd/Au (50/50 at. %) in the EDX map in Figure 4, which could imply significant grain growth for the Pd/Au (50/50 at. %) alloy. However, etching of the Pd/Au (50/50 at. %) sample shows that the wire is polycrystalline with a grain size of 10−30 μm (Figure S3). Additionally, EDX mapping of Pd/Au (50/50 at. %) after etching does not show Pt enrichment in the GBs (Figure S3). Grain size analysis of both poly- and quasi-monocrystalline versions of the Pd/Au samples shows that the polycrystalline wires are indeed polycrystalline after 10 days of heating at 900 °C (grain size of 10−30 μm) and that the quasi-monocrystalline wires maintain a much larger grain size (Figure S4). The low degree of GB diffusion is thus likely not to originate in grain growth.

Furthermore, the Pd and Au distributions in the Pd/Au alloys change during Pt-catchment; see Pd/(Pd + Au) ratio in Table 2. Comparing these ratios with the nominal compositions, there is less Au at the surface and more Au in the wire core after the experiment. EDX analysis of both poly- and monocrystalline Pd/Au heated in air at 900 °C without Pt-catchment shows that the Pd/Au ratio is homogeneous through the alloy, with no difference between the surface and the wire core (Figure S4, Table S1). It is possible that the oxygen content on the outer surface is not sufficiently high to cause bulk changes in composition, even if there are changes in the surface

https://doi.org/10.1021/acs.iecr.2c02852
Ind. Eng. Chem. Res. 2023, 62, 2478−2493

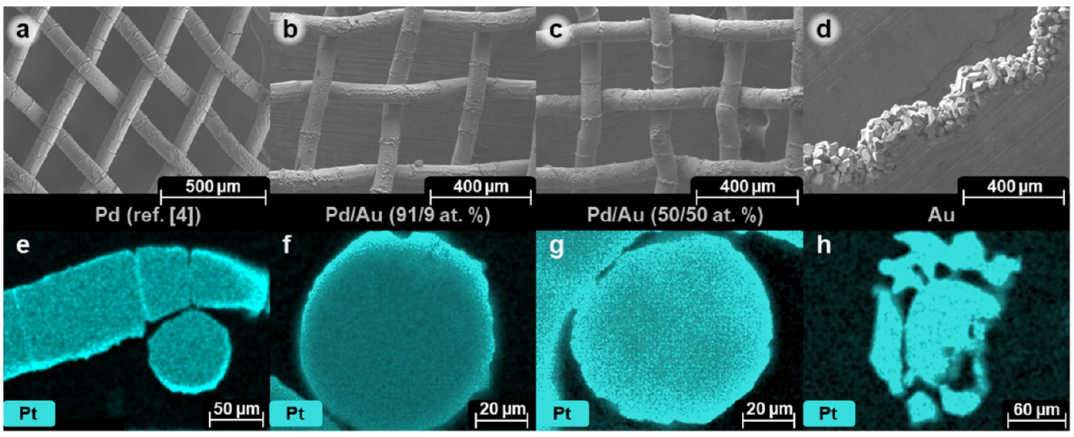

Figure 5. SEM images of the surface (top; a–d) and EDX-maps of the cross section (bottom; e–h) of the quasi-monocrystalline samples tested for Pt-catchment for 20 days at 900 °C in air; (a,e) Pd tested for 10 days (from Fjellvåg et al.[4]), (b,f) Pd/Au (91/9 at. %), (c,g) Pd/Au (50/50 at. %), and (d,h) Au. The curly shape of the Au wire originates from the fact that it was extracted from a woven net prior to the experiment. The experiments with the two Pd/Au samples were performed with the samples in the shape of nets (not isolated wires), as shown in the figure.

Table 4. Elemental Concentrations of Pd, Au, and Pt (at. %) from EDX Analysis of the Quasi-monocrystalline Samples after 20 Days of Pt-Catchment Experiments in Air at 900 °C

	Pd/Au(91/9 at. %)		Pd/Au(50/50 at. %)		Au
quasi-monocrystalline	Pt [at. %]	Pd/(Pd + Au) [at. %]	Pt [at. %]	Pd/(Pd + Au) [at. %]	Pt [at. %]
surface	12	95	15	57	10
cross section, 2 μm below surface	16	95	11	55	10
cross section, 12 μm below surface	2	91	3	48	10
cross section, center of wire core	0	92	3	50	10

composition. This implies that Pd is more strongly attracted than Au to the Pt on the surface during Pt-catchment. Furthermore, this may occur because Pt is captured in the alloy and diffuses into the solid and is not only present on the surface.

3.2.2. Quasi-monocrystalline (Preannealed) Pd/Au Alloys. To investigate the effect of Au content in the Pd/Au samples during Pt-catchment without the influence of grain boundaries, the polycrystalline samples were annealed to obtain quasi-monocrystalline configurations (see Materials and Methods Section and Figure 2). Subsequently, the Pt-catchment experiments were run for 20 days with the same conditions as used for the polycrystalline wires followed by mass change and ICP–OES analysis (Table 3). The mass change analyses underestimate again the Pt content compared to the ICP–OES analysis. The explanation is likely to be the same as for the polycrystalline samples, where a small piece near the front of the investigated wire spiral was sent for ICP–OES, while the entire wire was used for determining the mass changes. From ICP–OES, it can be seen that Pd/Au (50/50 at. %) and Au have collected the most Pt (~10 at. %), close to that of the corresponding polycrystalline wires. Pd/Au (91/9 at. %) collected slightly less Pt, ~7 at. %. This stands in contrast to reports on Pd,[4] which show a significantly lower Pt content after Pt-catchment experiments on quasi-monocrystalline wires (Table 3). Notably, both mass changes and ICP–OES indicate that all quasi-monocrystalline Pd/Au samples show improved Pt-catchment compared to quasi-monocrystalline Pd.

The quasi-monocrystalline grain structure can easily be seen for Pd/Au (91/9 at. %) and Pd/Au (50/50 at. %) in Figure 5a,c, where the GBs are visible as lines crossing the wire (see also analysis after etching in Figure 2). Considering the morphology of the samples, no grain reconstruction is observed for the two mixed Pd/Au alloys; only minor crystallites are formed on the surface at the locations most exposed to the gas stream (Figure 5a,b). For Au, however, the morphological changes resemble those of the polycrystalline wire (Figure 5c).

Considering the wire cross sections (Figure 5), we see a clear trend in Pt distribution. For Pd/Au (91/9 at. %), Pt mainly covered the surface, while it penetrated much deeper into the Pd/Au (50/50 at. %) alloy. For pure Au, Pt once again has a homogenous distribution in the entire sample. Quantitative EDX analysis supports these results (Table 4), showing that the three samples have 0, 3, and 10 at. % Pt in the wire core, increasing with Au content in the sample. The increased Pt concentration in the wire core correlates very well with our expectations of a more rapid bulk diffusion for the Au-rich samples. An approximate diffusion coefficient (Table S4c) is calculated from the EDX data point at the deepest point into the wires with a reliable Pt concentration, and they are in the range of the approximated diffusion coefficients (Table S4a). Interestingly, the Pt concentration is equal for both poly- and quasi-monocrystalline Pd/Au (50/50 at. %) alloys, indicating that Pd/Au (50/50 at. %) is mainly driven by bulk diffusion and not GB diffusion. This is probably related to the improved bulk mobility caused by adding Au to the alloy, as discussed in the introduction.

Also for the quasi-monocrystalline samples, there is a small variation in the Pd/(Au + Pd) ratio at different locations in the wire cross section; there is more Pd (less Au) near the surface (Table 4), similar to the polycrystalline samples (Table 2). Because we have not observed a similar change in the Pd/(Pd + Au) ratio in Pd/Au samples heated for 10 days in air at 900 °C, it is likely that Pd has a higher preference for mixing with Pt during Pt-catchment experiments.

https://doi.org/10.1021/acs.iecr.2c02852
Ind. Eng. Chem. Res. 2023, 62, 2478–2493

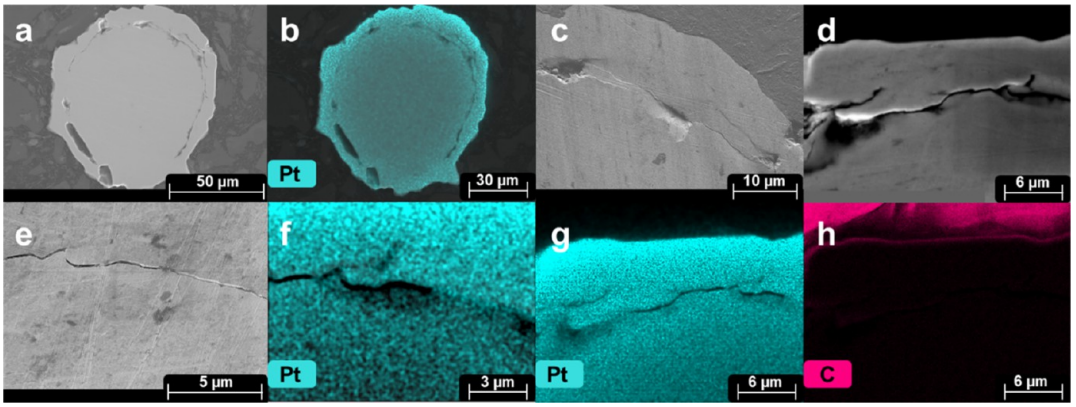

Figure 6. SEM images and EDX maps of the Pd/Au (50/50 at. %) sample after 20 days Pt-catchment at 900 °C, which show the linear void 10−15 μm below the wire surface. The cyan EDX maps (b,g,h) show Pt, while the dark pink EDX map (i) shows C (carbon).

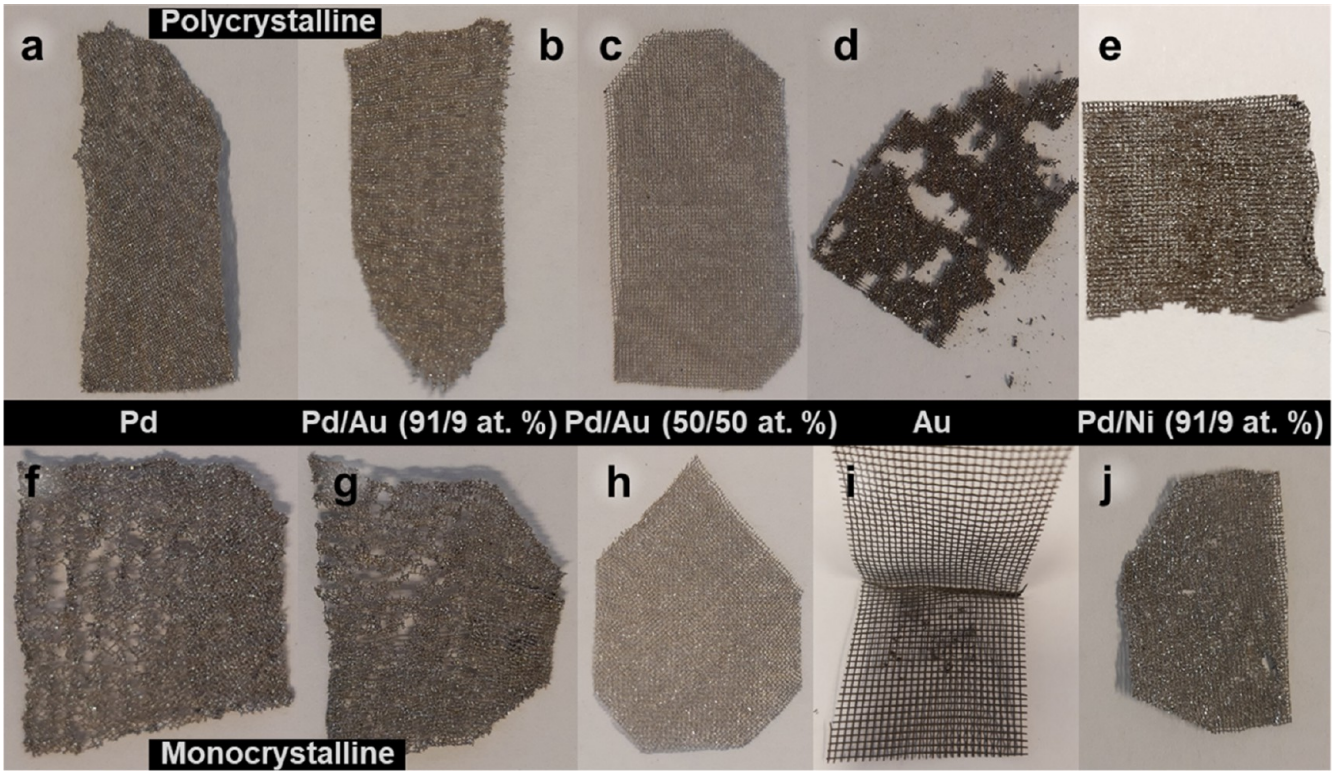

Figure 7. Photos of the sample nets after the experiment in the industrial plant. The top row (a−e) shows the polycrystalline samples: (a) Pd, (b) Pd/Au (91/9 at. %), (c) Pd/Au (50/50 at. %), (d) Au, and (e) Pd/Ni (91/9 at. %). The bottom row (f−j) shows the quasi-monocrystalline samples: (f) Pd, (g) Pd/Au (91/9 at. %), (h) Pd/Au (50/50 at. %), (i) Au (the sample is a small black powder on the megapyr net in the picture), and (j) Pd/Ni (91/9 at. %). Figure S6 shows how the sample nets looked before the experiment.

In the analysis of the Pd/Au (50/50 at. %) sample, one of the samples shows a difference in the wire cross section. A very long and thin (almost linear) void appeared 10−15 μm below the wire surface and extended along a large section of the sample; see Figure 6. The void is different from the other samples analyzed because it is shaped circularly along with the shape of the wire surface, and it is very thin at certain locations. EDX analysis shows a gradually reducing Pt concentration from the surface and past the void, inward into the sample. There is generally a lower concentration of Pt on the inside of the void (Table S3 and Figure S5) but not a larger difference than the expected Pt concentration versus depth seen in other samples (Table 4). Unlike several other voids/pores, there is no carbon from the casting material present in the thin linear pore (Figure 6i). The origin of the pore is unknown. One option is that internal voids were formed by agglomeration of vacancies. Alternatively, it is a mechanical situation caused by a difference in thermal expansion coefficients causing the wire to crack. The outer part of the wire is Pt-rich, which has a lower thermal expansion coefficient compared to Pd/Au,[28,30] and thus cannot shrink as much as the Pd/Au core of the wire during cooling from 900 °C to room temperature. From the reported thermal expansion coefficients, a difference in ∼0.2 μm is calculated for the cooling of a 76 μm Pd/Au (50/50 at. %) wire compared to Pt.

3.3. Industrial Scale Experiments. To explore the feasibility of using the Pd/Au alloys at industrial plant conditions, the same Pd/Au samples that were used in the laboratory experiments were tested in a 5 month long campaign

https://doi.org/10.1021/acs.iecr.2c02852
Ind. Eng. Chem. Res. 2023, 62, 2478−2493

Table 5. Normalized Mass Changes (Left) of the Samples Tested for Pt-Catchment in the Industrial Plant for 5 Months and the Corresponding ICP−OES Results (Right)[a]

	mass change	ICP−OES				
polycrystalline	Δm [mg]	m(Pt) [mg]	Pt [at. %]	Pd [at. %]	Au [at. %]	Rh [at. %]
Pd	8	19	10	90		0.2
Pd/Au(91/9 at. %)	12	20	10	80	10	0.2
Pd/Au(50/50 at. %)	26	11	5	47	48	0.0
Au	−34	4	3		97	0.0
Pd/Ni(91/9 at. %)	0.2	0.0	5	95		
	mass change	ICP−OES				
quasi-monocrystalline	Δm [mg]	m(Pt) [mg]	Pt	Pd	Au	Rh
Pd	10	23	12	88		0.2
Pd/Au(91/9 at. %)	12	20	10	79	10	0.2
Pd/Au(50/50 at. %)	25	8	4	48	49	0.0
Au	−91	2	2		98	0.1
Pd/Ni(91/9 at. %)	8	27	15	85		0.2

[a]The column named "m(Pt) [mg]" is the mass of Pt calculated from the ICP−OES analyses.

Table 6. Calculations Based on the Obtained Mass Changes and ICP−OES Results for the Samples Tested for Pt-Catchment in the Industrial Plant[a]

polycrystalline	Pd before/Pd after (at. %)	Au before/Au after (at. %)	m(Pt)/$\Delta(m)$	metal-loss[wt %]
Pd	88		2.49	11
Pd/Au(91/9 at. %)	89	118	1.64	7
Pd/Au(50/50 at. %)	108	111	0.41	−11
Au		77	−0.11	23
Pd/Ni(91/9 at. %)	96		38.81	9
quasi-monocrystalline	Pd before/Pd after (at. %)	Au before/Au after(at. %)	m(Pt)/$\Delta(m)$	metal-loss[wt %]
Pd	87		2.27	12
Pd/Au(91/9 at. %)	88	121	1.58	6
Pd/Au(50/50 at. %)	110	111	0.32	−12
Au		45	−0.02	55
Pd/Ni(91/9 at. %)	84		3.54	19

[a]The first two columns show the ratio of the moles of Pd and Au in the sample before and after the experiment, calculated from the ICP−OES data. Column no. 3 shows the ratio of the Pt content measured from ICP−OES to the mass increase, and the final column shows the metal loss of Pd and Au from the original alloys through the experiment.

in one of the industrial reactors for ammonia oxidation at Yara International (Herøya, Norway). Both poly- and quasi-monocrystalline nets of Pd, Pd/Au (91/9 at. %), Pd/Au (50/50 at. %), Au, and Pd/Ni (91/9 at. %) were exposed (Figure S6).

3.3.1. Preparation and Unpacking of the Samples Exposed in the Industrial Plant. Before the experiment, the samples were carefully prepared (see Materials and Methods Section) to ensure that only the gas atmosphere would interact with the samples and not physical objects (oxide or metallic particles, etc.). Upon unpacking of the samples after the 5 month campaign, clear visual differences between the samples are observed (Figure 7). Most obviously, the Au nets are almost completely destroyed, and only a small brittle piece resembling a net remains. Of the Pd-based alloys, the Pd/Au (50/50 at. %) samples are visually almost unaffected by the experiment (Figure S6), while the rest show varying degrees of morphological changes. The nets of the quasi-monocrystalline samples are in a slightly worse condition after the experiment compared to the corresponding polycrystalline samples.

3.3.2. Mass Changes and ICP−OES Analysis of the Samples Exposed in the Industrial Plant. Careful sample preparation allowed us to determine the mass changes after a duration of 5 months in the plant with high accuracy. Because all samples were of different sizes, the mass changes were normalized relative to the sample volume of the Pd net. The normalized mass changes are reported in Table 5. Pd/Au (50/50 at. %) has the highest normalized mass increase, far above the other samples. Considering the samples, the normalized mass increase goes in the following order

$$\text{Pd/Au (50/50 at. \%)} \gg \text{Pd/Au (91/9 at. \%)} > \text{Pd} > \text{Pd/Ni (919 at. \%)} \gg \text{Au}$$

The polycrystalline Pd/Ni (91/9 at. %) wire is an outlier in all analyses, probably because it was treated in a different sample pack in the plant, and is therefore not carefully considered in the analysis. For the quasi-monocrystalline Pd/Ni (91/9 at. %) sample, the slightly lower mass increase of this sample compared to Pd is probably related to the loss of Ni.[3] Both Au samples show a significant mass loss, which is not surprising, considering the appearance of the sample after the experiment (Figure 7). There is generally a small difference between the mass changes of the polycrystalline and quasi-monocrystalline samples.

After unpacking the samples, one piece of each sample was sent for ICP−OES analysis. The results from the ICP−OES analyses are reported in Table 5. First, the alloys have captured different amounts of Pt, in addition to some minor quantities of Rh. However, the Pt concentrations from ICP−OES follow a quite different trend from the observed mass changes (Table 5)

https://doi.org/10.1021/acs.iecr.2c02852
Ind. Eng. Chem. Res. 2023, 62, 2478−2493

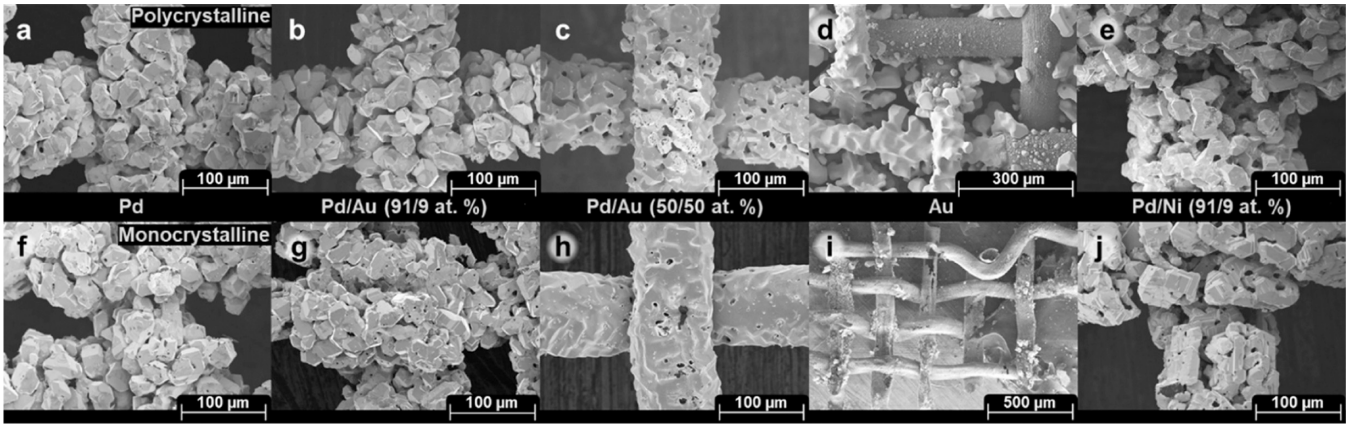

Figure 8. SEM images of the surface of the different samples after the industrial plant experiment. The top row (a–e) shows the polycrystalline samples: (a) Pd, (b) Pd/Au (91/9 at. %), (c) Pd/Au (50/50 at. %), (d) Au, and (e) Pd/Ni (91/9 at. %). The bottom row (f–j) shows the quasi-monocrystalline samples: (f) Pd, (g) Pd/Au (91/9 at. %), (h) Pd/Au (50/50 at. %), (i) Au, and (j) Pd/Ni (91/9 at. %).

$$\text{Pd/Ni (91/9 at. \%, pre annealed)} > \text{Pd} \approx \text{Pd/Au (91/9 at. \%)} > \text{Pd/Au (50/50 at. \%)} > \text{Au}$$

The Pd/Au (50/50 at. %) alloys have a surprisingly low Pt concentration, considering the fact that these samples had the highest mass increase. Also, all Ni had been lost from the Pd/Ni (91/9 at. %) alloys. It is surprising that the quasi-monocrystalline Pd/Ni (91/9 at. %) sample has a higher Pt content than all other samples, including Pd, as previous lab-scale investigations show that Ni does not participate in the Pt-catchment process.[3,4] Perhaps there is an effect from the industrial conditions/gas mixture, which should be investigated more carefully.

From the atomic percentages provided by ICP–OES (Table 5), we can calculate the molar amount of Pd and Au in the alloys by using the mass of the samples and assuming the samples are homogeneous. By comparing this with the original atomic content in the samples, we can calculate the change in Pd and Au contents through the experiment; see Table 6. For Pd and Pd/Au (91/9 at. %), the Pd content is reduced significantly, indicating a Pd loss (Table 6, metal loss). This correlates well with previous reports of Pd loss from Pd-based catchment gauzes when operated in industrial conditions.[4]

For Pd/Au (50/50 at. %), we surprisingly observe an increase in the absolute content (mass) of both Pd and Au during the experiment. This is obviously not possible as Au cannot be captured during the experiment. It also seems unlikely to have significant Pd-catchment originating from Pd lost from the industrially installed Pd/Ni gauzes. A small increase in the Au content is also measured for Pd/Au (91/9 at. %). These results are unexpected, and they cannot originate from Pt-catchment. Along with Mikrolab Kolbe, who performed the ICP–OES analyses, we attempted to understand the origin of the unexpectedly high Pd and Au contents by remeasuring and by searching for other elements through element screening. Only Al and Cr are identified as additional elements, with a concentration in the range of 100–200 ppm, far below the concentrations needed to explain the observed mass gain and low Pt concentration. On the positive side, the Pd/Au (50/50 at. %) samples do not show any Pd loss, which is one of the main drawbacks of the industrial Pd/Ni (91/9 at. %)-catchment system.[3] This finding is similar to the results from Holzmann,[5] showing that the Pd loss is lower for the Au-rich alloys, although not completely absent.

3.3.3. SEM/EDX Analysis of the Samples Exposed in the Industrial Plant. SEM investigation of the sample surfaces reveals that the different compositions show very different morphological changes; see Figure 8. The reconstruction of the samples are in general very homogeneous over the entire sample; there is only a small difference between the *up* (gas inflow side) and the *down* (gas out-flow side) sides for some samples, while different locations on the net are very similar in shape (Figures S7 and S8). Both the poly- and quasi-monocrystalline versions of Pd and Pd/Au (91/9 at. %) nets and the polycrystalline Pd/Ni (91/9 at. %) net show a structural reconstruction similar to the reconstruction described in the previous chapter on laboratory samples (Section 3.2). Pd/Au (50/50 at. %) looks similar as in the laboratory experiments, with a low degree of grain reconstruction. Interestingly, the weave has become tighter for the Pd-rich samples compared to Pd/Au (50/50 at. %), that is, the distance between the center of each wire is smaller for the Pd-rich samples than for Pd/Au (50/50 at. %) (Figures S7 and S8). The Au nets are almost unrecognizable after the campaign and is in no way similar to the laboratory samples, indicating that they have reacted with the surroundings during the experiment. Finally, the Pd/Ni (91/9 at. %, quasi-monocrystalline) sample also reconstructs, but the crystallites are larger and have a shape different from the other samples. Reconstruction of the quasi-monocrystalline samples was not observed in the laboratory experiments with durations up to 20 days (Section 3.2), but clearly, the long-term industrial campaign of 5 months forces also the quasi-monocrystalline samples to reconstruct during Pt-catchment. Whether this occurs solely due to prolonged exposure times combined with only Pt-catchment, or with relation to the extreme gas/temperature conditions as well, remains an open question. It would be highly desirable to understand the driving force behind going from the large crystallite size at the beginning of the experiment to the smaller isolated crystals as observed at the end of the experiment.

To further investigate the unexplainably large mass gain of the Pd/Au (50/50 at. %) samples compared to the low Pt concentration measured by ICP–OES, careful EDX quantification was performed; see Table 7. The surface Pt concentration is highest for Pd/Ni (91/9 at. %), slightly higher than those for the Pd and Pd/Au (91/9 at. %) samples, correlating well with ICP–OES (Table 5). For Pd/Au (50/50 at. %), the surface Pt concentration is much lower in the range of the Pt concentration

https://doi.org/10.1021/acs.iecr.2c02852
Ind. Eng. Chem. Res. 2023, 62, 2478–2493

Table 7. EDX Quantification of the Samples Tested as Pt-Catchment Materials in the Industrial Plant[a]

	Pt/(Pd + Pt + Au)[at. %]			Pd/(Pd + Au)[at. %]		
polycrystalline	surface	CS, edge	CS, center	surface	CS, edge	CS, center
Pd	12	11	5			
Pd/Au (91/9 at. %)	13	7	4	94	92	91
Pd/Au (50/50 at. %)	6	4	2	60	59	57
Au	3			19[b]		
Pd/Ni(91/9 at. %)	6	9	4			
	Pt/(Pd + Pt + Au)[at. %]			Pd/(Pd + Au)[at. %]		
quasi-monocrystalline	surface	CS, edge	CS, center	surface	CS, edge	CS, center
Pd	15	10	4			
Pd/Au (91/9 at. %)	15	12	6	94	92	90
Pd/Au (50/50 at. %)	6	4	2	61	59	56
Au	5			53[b]		
Pd/Ni(91/9 at. %)	19	11	5			

[a]All quantifications are taken from the *up* side (meeting the incoming gas), which is the most Pt-rich side of the alloys shown in Figure 9. CS = cross section of the wire. [b]For clarification, Pd is captured during the industrial experiment as the Au wire did not contain Pd at the start of the experiment.

determined from ICP−OES (Table 5). EDX quantification at several locations over the entire sample surface on both the *up* and *down* sides of the net shows a homogeneous Pt distribution in the range of 6−7 at. % Pt on the *up* side and 4−5 at. % Pt on the *down* side. EDX analysis supports the low Pt concentration determined from ICP−OES for the Pd/Au (50/50 at. %) samples. Only ∼32% of the mass increase of the Pd/Au (50/50 at. %) samples can be attributed to Pt-catchment.

EDX mapping of the wire cross section (Figure 9) shows how the Pt distribution is for the different samples and how the bulk morphology of the wires has changed. The trend of the surface reconstruction is also visible in the sample cross sections, where Pd, Pd/Au (91/9 at. %), and Pd/Ni (91/9 at. %) alloys show complete reconstruction, forming porosity all the way from the wire surface into the wire core. Pd/Au (50/50 at. %) also shows a certain degree of porosity, but the main part of the wire is still intact as a solid piece. Again, there is a negligible difference between the quasi-monocrystalline and polycrystalline samples.

When it comes to the Pt content, most samples show a small difference between the upstream (*up*) and downstream (*down*) sides of the sample, where the *up* side is richer in Pt (brighter color in Figure 9). For all samples, the Pt concentration is highest on the surface and reduces toward the wire center as well as to the center of each grain, see Table 7. Due to the high mobility in the Pd/Au (50/50 at. %) alloy (Table S4), we could have expected it to have the highest Pt content in the wire core. However, the Pd-rich samples have the highest Pt concentration in the wire core, most likely because of the restructuring of the wire. For all of the Pd/Au samples, the Pd/(Pd + Au) ratio is higher near the surface, which also corresponds to the most Pt-rich locations (Figure S9). EDX analysis also indicates (nonconclusively) that the Pt-rich locations inside the sample (such as the GBs) also have a higher Pd/(Pd + Au). This indicates that Pd has a higher preference than Au to be near Pt during Pt-catchment.

For the Pd/Au (50/50 at. %) sample, the EDX map shows a weak color pattern crossing the wire at certain locations (Figure 9c,g). A similar feature is also weakly seen on the other samples. We can speculate that the brighter parts of the pattern correspond to grain boundaries, while the darker parts correspond to the center of grains, as observed for the laboratory samples above (Section 3.2).

Both the poly- and quasi-monocrystalline Au samples reacted strongly with the environment during the industrial campaign. Both the gas atmosphere and the megapyr support may have reacted with the sample; 1−1.5 wt % Au is found in the megapyr used to hold the Au sample in the sample pack during the experiment. SEM imaging (Figure 8i) and EDX mapping (Figure 10) of the polycrystalline sample shows that parts of the wire remain metallic (left side in EDX-maps), while the other parts seem to be dominated by an oxide (right part in EDX map). The metallic part of the wire is dominated by noble metals and contain mainly Pt, Au, and Pd (Figure 10a−c). Surprisingly, there is a significant concentration of Pd in the metallic parts of the polycrystalline Au sample. At these locations, we find 10−20 at. % Pd and only 2−3 at. % Pt from the EDX analysis. ICP−OES analysis shows 3.8 at. % Pd and 2.9 at. % Pt over a large sample piece, and the rest is Au. The obtained Pd in this alloy has possibly been captured from the volatile loss of Pd from the industrial Pd/Ni-catchment system used in the plant. This

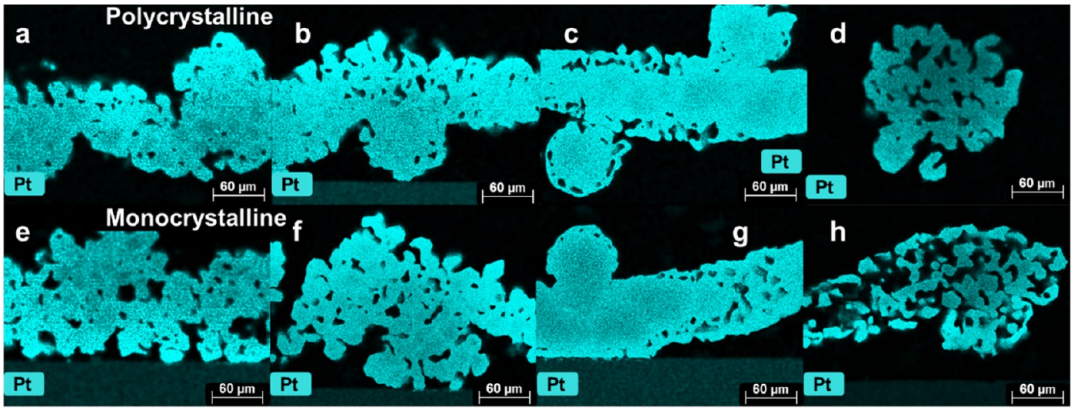

Figure 9. EDX maps of the samples tested for Pt-catchment in the industrial plant, except for Au which could not be prepared as a cross section. The top row (a−d) shows the polycrystalline samples: (a) Pd, (b) Pd/Au (91/9 at. %), (c) Pd/Au (50/50 at. %), and (d) Pd/Ni (91/9 at. %). The bottom row (e−h) shows the quasi-monocrystalline samples: (e) Pd, (f) Pd/Au (91/9 at. %), (g) Pd/Au (50/50 at. %), and (h) Pd/Ni (91/9 at. %).

https://doi.org/10.1021/acs.iecr.2c02852
Ind. Eng. Chem. Res. 2023, 62, 2478−2493

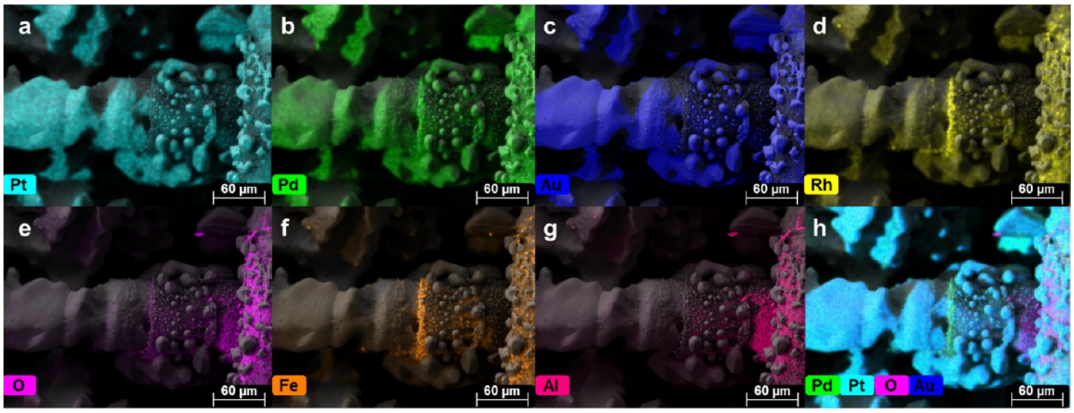

Figure 10. EDX maps on top of a SEM image of the polycrystalline Au sample tested for Pt-catchment in the industrial plant. The images focus on a very strange intersection between metallic and oxide-based regions (SEM image shown in Figure 8i). The elements scanned for and shown in the figure are (a) Pt, (b) Pd, (c) Au, (d) Rh, (e) O, (f) Fe, (g) Al, and (h) Pd, Pt, O, and Au.

indicates that Au may reduce the Pd loss, which may be why the Pd loss is very low from the Pd/Au (50/50 at. %) alloy. The oxide parts of the polycrystalline Au sample contain a mixture of several elements, such as Fe, Al, Rh, and O, but we have not been able to identify exactly which oxides, in terms of composition and atomic arrangement.

The main findings from the industrial plant experiment are summarized in Figure 11, showing how Pt-catchment, total mass change, Pd loss, and wire swelling correlate with the Pd/Au composition.

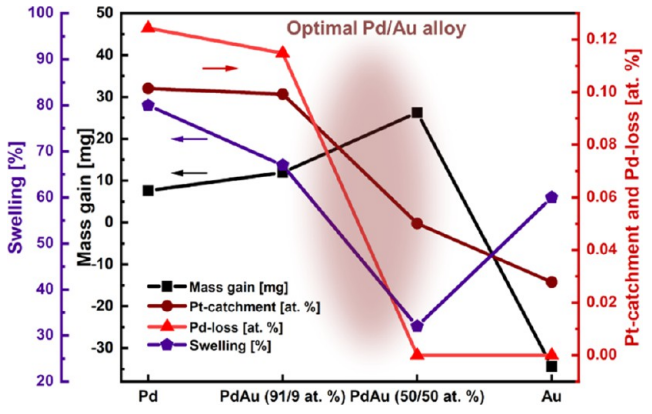

Figure 11. Summary of the mass gain [mg], Pt-catchment [at. %], Pd loss [at. %], and wire swelling [%] for the Pd/Au samples treated in the industrial plant for 5 months. The data connected to wire swelling of Au is taken from the laboratory experiments. The composition range predicted as the optimal Pd/Au alloy for Pt-catchment is shaded dark red in the figure.

4. DISCUSSION

The grain reconstruction process of polycrystalline Pd and Pd/Ni (91/9 at. %) wires has recently been described as a corrosion process caused by gas-phase platination.[4] It is said that inward Pt diffusion is limited due to slow bulk diffusion and that inward Pt diffusion and outward Pd diffusion take place mainly through the GBs.[4] In relation to the present work, Pd/Au alloys are utilized to perform Pt-catchment on alloys with improved bulk diffusion relative to Pd. We assume that GB diffusion is unaffected by adding Au to the alloy, which implies that the GB-diffusion/bulk-diffusion ratio is reduced for the Pd/Au alloys relative to Pd and Pd/Ni (Table S4).

4.1. Effect of Enhanced Bulk Diffusion on Grain Reconstruction of Polycrystalline Pd-Based Pt-Catchment Systems. With respect to grain reconstruction of the polycrystalline wires, we have four major observations.

1. Grain reconstruction is reduced with increasing Au content, up to Pd/Au (50/50 at. %) (Figure 4).
2. The Pt content in the core of the quasi-monocrystalline samples increases with increasing Au content (Table 4).
3. The Pt content in the core of the poly- and quasi-monocrystalline Pd/Au (50/50 at. %) samples is equal (Table 4).
4. GB diffusion is less pronounced for samples with higher Au content (Figure 4).

The results demonstrate that the grain reconstruction process is reduced by improving the bulk diffusion of the Pt-catchment alloy. In addition, we have performed diffusion simulations using the diffusion model reported by Fjellvåg et al.[4] and the estimated diffusion coefficients for Pd/Au (Table S4). Au enrichment generally enhances the diffusion-based Pt-absorption capacity of the samples when compared in the same time window (e.g., 10 days). From a purely diffusional perspective, the diffusion model shows that the monocrystalline Pd/Au (50/50 at. %) sample absorbs more Pt than the polycrystalline Pd/Au (91/9 at. %) sample (Figure S10). Considering this along with point 3 above, the GBs become a less important diffusion path for the Au-rich samples.

In the following, we will implement the effect of improved bulk diffusion, introduced by Au alloying, to the already suggested mechanism on grain reconstruction proposed for Pd (and Pd/Ni) wires by Fjellvåg et al.;[4] see Figure 12. We assume that different Pd/Au samples have the same GB diffusion rate, but bulk diffusion is enhanced in Au-enriched alloys (black and purple arrows). During a Pt-catchment experiment, the surface is quickly covered with Pt, and the diffusion process begins. For the Pd-rich wire [such as Pd/Au (91/9 at. %)], GB diffusion is much faster than bulk diffusion, and the grain reconstruction mechanism occurs, as suggested by Fjellvåg et al.[4] For the Au-rich alloy [such as Pd/Au (50/50 at. %)], the Au content enhances bulk diffusion relative to GB diffusion (Table S4) and causes the GB/bulk ratio to be reduced by over 1 order of magnitude, thus reducing the grain reconstruction. This also causes the grain structure of the Au-rich sample to be less

https://doi.org/10.1021/acs.iecr.2c02852
Ind. Eng. Chem. Res. 2023, 62, 2478−2493

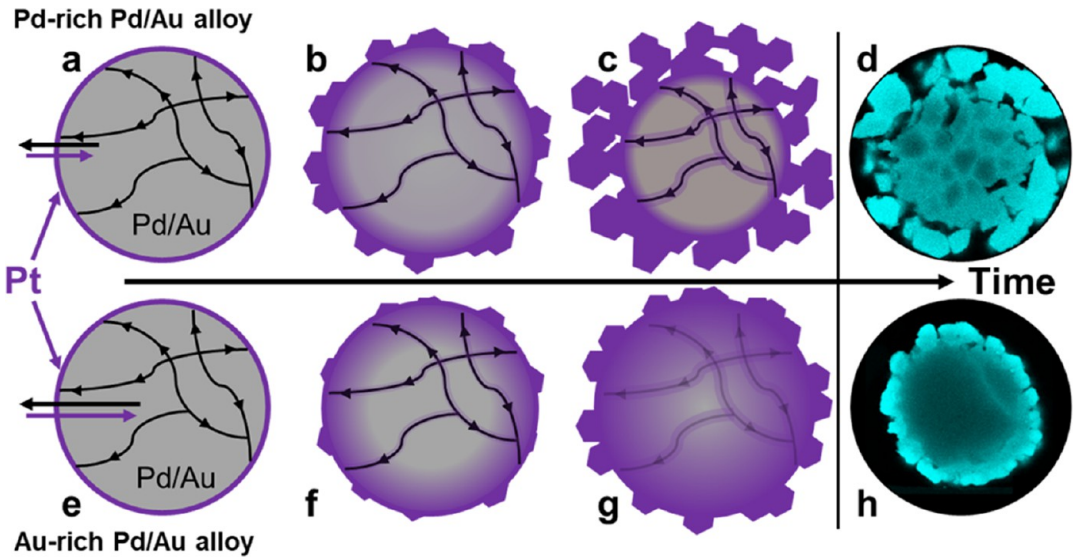

Figure 12. Suggested mechanism for the suppression of grain reconstruction in polycrystalline Pd/Au alloys during Pt-catchment. The figure is a modified version of the one published by Fjellvåg et al.[4] The top part of the figure shows a (a) model polycrystalline Pd/Au sample with Pd excess, (b) Pd/Au sample early in the Pt-catchment process, (c) Pd/Au sample late in the Pt-catchment process, and (d) EDX map of a Pd/Au (91/9 at. %) sample. The bottom part of the figure shows a (e) model polycrystalline Pd/Au sample with a large Au content, (f) Pd/Au sample early in the Pt-catchment process, (g) Pd/Au sample late in the Pt-catchment process, and (h) EDX map of a Pd/Au (50/50 at. %) sample.

important as poly- and quasi-monocrystalline Au-rich samples behave very similarly. However, it is important to note that Au is an exception and behaves differently (see Section 3.2).

An alternative description is that for the current conditions (Pt-catchment in air at 900 °C), the wire seeks to obtain equilibrium and the most favorable alloy composition as fast as possible. For the Pd-rich wire, the fastest transportation route is GB/surface diffusion, which implies that a high surface area and reconstructed crystals are beneficial. For an Au-rich alloy, the bulk diffusion is sufficiently fast to remove this driving force, that is, an increase in the surface area is not equally necessary to obtain alloy equilibrium fast. However, this does (again) not explain the reconstruction of the pure Au wire.

4.2. Restructuring of Au during Pt-Catchment. With respect to Pt-catchment on Au, we have three main findings:

1. Au restructures in the same way as both poly- and quasi-monocrystalline samples in the laboratory experiments (Figures 3 and 5).
2. The restructuring of the Au wires occurs in a different manner than for Pd, Pd/Ni, and Pd/Au alloys. The crystals seem to grow onto the surface, while the Pd-rich alloys seem to reshape the already present grain structure (bulk grain exchange GBs for the surface) (Figure 3).
3. The Au wire core shrinks during the experiment but remains morphologically intact and alloyed with Pt even after long durations (Figures 4 and S1).

With respect to why the poly- and quasi-monocrystalline samples behave so similar, we consider two possibilities; (1) the polycrystalline sample shows rapid grain growth during the experiment, causing both samples to be, in practice, monocrystalline during the experiment (supported by onset of grain growth at 400 °C[38]), or (2) the GB diffusion does not play a role in this system, despite it being rapid, because bulk (and surface) diffusion is sufficiently fast to transport all Pt throughout the wire sample. Either way, GB diffusion is not important for Pt-catchment on Au.

Unfortunately, we can only speculate on the underlying reasons for the different restructuring of Au compared to Pd/Au. For Au, the wire core remains morphologically intact after prolonged exposure to gaseous PtO_2 in contrast to the Pd-based samples. Au shows a homogeneous Pt concentration limit of ∼10 at. % Pt throughout the sample, obtained within 20 days of Pt-catchment (Tables 1−4). A maximal Pt-catchment of only 10 at. % in the Au−Pt system is significantly lower than that obtained in the Pd−Pt system[4,39] (20−30 at. %). It may be that the reconstruction of Au only occurs as long as the system captures Pt, that is, while the wire has not yet reached the Pt concentration limit. We suggest that when Pt is captured, it nucleates and forms crystals on the Au wire surface simultaneously as a portion of the Pt atoms diffuses into the Au wire. The Pt atoms/clusters on the surface immediately attract Au as the crystallites are shown only to contain a limiting Pt concentration of ∼10−12 at. % early in the experiment (Tables 1−4). The reason why the Au wire core is able to shrink in size instead of restructuring is hard to answer; we speculate that it is due to the overall rapid diffusion and mobility of Au due to the proximity to the melting point. The process stops at the point when the wire is saturated in Pt. Exactly why the crystallites are formed on the surface is difficult to answer. We propose two alternatives:

1. Nucleation and growth of new crystals may be favorable during this alloying process because it exposes clear faceted crystals (low-energy surfaces) rather than the regular wire surface. In this mind set, the wire core should also reconstruct, unless the restructuring process only occurs until Pt-catchment stops (when the wire is saturated in Pt).
2. The Pt concentration on the wire surface is too large to handle by the bulk/GB diffusion into the wire core. This causes crystallization to occur, with the purpose of increasing the surface area and facilitating more Pt-catchment (similar to Pt-catchment on polycrystalline Pd). The crystal growth process on the surface is possible

https://doi.org/10.1021/acs.iecr.2c02852
Ind. Eng. Chem. Res. 2023, 62, 2478−2493

because the rapid diffusion of Au can provide many Au atoms in a short time.

Certainly, a combination of both mechanisms may be the real scenario, and further investigations are recommended.

4.3. Restructuring of the Quasi-monocrystalline Samples. With respect to the quasi-monocrystalline samples, we have two important observations:

1. In the 5 month industrial experiment, all Pd-containing quasi-monocrystalline samples restructure in the same way as the polycrystalline ones (Figure 8).
2. In the laboratory experiments, one of the cross sections of the quasi-monocrystalline Pd/Au (50/50 at. %) samples show an internal void similar to our expectations of a Kirkendall void (Figure 6).

In a practical perspective, there is no benefit from using quasi-monocrystalline samples for industrial scale Pt-catchment since they also restructure, only taking more time. However, it is highly desirable to understand the mechanism behind the restructuring to develop improved Pt-catchment systems. The mechanism describing grain reconstruction (Fjellvåg et al.[4] and Section 4.1) does not include the monocrystalline versions of the Pd and Pd/Au samples, but the concept of both bulk and GB Kirkendall effect, which is known to cause internal voids in diffusion processes,[19−26] was discussed by Fjellvåg et al.[4] In Pd and Pd/Ni, the outwars flux of Pd during Pt-catchment caused an inward flux of vacancies (due to slow Pt diffusion), which may agglomerate into internal voids. This is equally likely to occur during Pt-catchment on Pd/Au alloys. Pd/Au (50/50 at. %) shows a different-looking internal void in one of the sample cross sections, close to our expectations of an internal Kirkendall void (Figure 6). The SEM images and the EDX maps indicate that this is not open porosity, and the void follows the circular shape of the wire surface. This is a strong indication that the formation of Kirkendall voids is part of the mechanism for the restructuring of the Pd-based wires during Pt-catchment.

The fact that the quasi-monocrystalline samples restructure indicates that they have an energetic gain by restructuring from a wire with a large grain structure (50−200 μm = quasi-monocrystalline) to a mixture of several smaller and clear faceted crystals (20−50 μm) similar to Au. There may be an energy gain from different surface exposures. Both the long duration of the industrial experiment (5 months) and the extreme gas conditions could be the factors determining the reconstruction.

We suggest that the formation of Kirkendall voids is the first step in the restructuring of the quasi-monocrystalline Pd-based wires (Figure 13b). The restructuring starts with a net inward diffusion of vacancies because of the more rapid outward diffusion of Pd compared to the inward diffusion of Pt (Figure 13a). This also applies to Pd/Au, where Pd is enriched at Pt-rich locations, that is, Pd moves toward Pt, while Au remains approximately still. With time (Pt-catchment), the internal void establishes contact with the surface (Figure 13c) and transforms into an open pore (Figure 13d). At this stage, it is natural to assume that Pt-catchment also occurs inside the pore and that recrystallization of the entire surface (now with a much higher surface area) occurs in order to minimize the surface energies, that is, create clear faceted crystals. Similar to the grain reconstruction process, this is probably a self-repeating process that will continue for as long as there is Pt-catchment and until the entire wire is restructured. It may be that during Pt-catchment, the noble metal wires, regardless of the grain

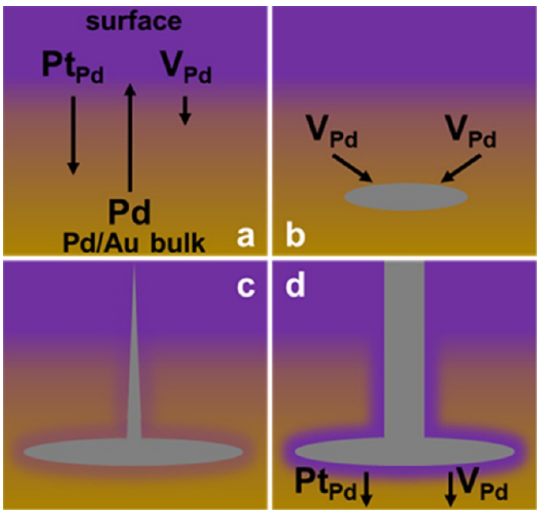

Figure 13. Illustration of (a) diffusion of the different species (arrow indicates diffusion flux), (b) formation of an internal Kirkendall void, (c) Kirkendall void growing toward the wire surface, and (d) Kirkendall void with open porosity that starts to facilitate Pt diffusion even deeper into the sample.

structure, desire to change their morphology to expose only the low-energy orientations toward the surface and that the bulk/surface diffusion of Pt facilitates this restructuring.

Finally, it should be noted that the Pd/Au (50/50 at. %) sample resists complete restructuring. This sample has an intermediate Au content, in between Au- and Pd-rich compositions, which have two distinct restructuring mechanisms:

- Pd-rich [e.g., Pd/Au (91/9 at. %)] alloys create internal voids and reshape the already present wire structure into several separated crystals.
- Au grows new crystals on top of the wire surface, and no internal voids are formed.

A key difference between the Pd-rich and Au samples is the different diffusion rates and reconstruction with different mechanisms. We consider the possibility that the poly- and quasi-monocrystalline Pd/Au (50/50 at. %) samples are affected by both mechanisms and, consequently, goes through only a small reconstruction. We speculate it is the rapid Pt transport to the wire core that suppresses the grain reconstruction (as in the Pd-rich wires) simultaneously as the growth of surface crystals (as on Au) is suppressed because of the higher melting point when Pd is present in the alloy. Perhaps there is a range of Pd/Au compositions that display this kind of mechanism, in between those of the end members in the system, with different properties in other aspects related to Pt-catchment (higher Pt saturation and low Pd loss).

4.4. On the Effect of Mass Catchment versus Mass Loss on Wire Restructuring. One very interesting observation by Fjellvåg et al.[3] is that Pd/Ni (91/9 at. %) shows a significant NiO loss from the wire in wet air, and no internal voids appeared. There was only a small reconstruction of the surface (surface roughness). In this scenario, there is also outward diffusion (of NiO) from inside the wire to the surface. However, in contrast to Pt-catchment, no internal porosity appeared. The only difference we can imagine between these scenarios is the surface diffusion of Pt during Pt-catchment, which is absent during Ni loss from Pd/Ni in wet air. The surface diffusion of Pt and its desire to create clear faceted crystals on the surface seem to be

https://doi.org/10.1021/acs.iecr.2c02852
Ind. Eng. Chem. Res. 2023, 62, 2478−2493

the key factors causing the final restructuring. This comparison between Ni loss and Pt-catchment is recommended for further investigations.

4.5. Comment on the Mechanism for Pt-Catchment from PtO_2. Another topic that is insufficiently addressed in previous literature is the mechanism for Pt-catchment onto a material surface. How does Pt react from the gas-phase molecule PtO_2 and become metallic Pt in an alloy with Pd and Au? Fierro et al.[10] suggested that trace amounts of NH_3 work as a reducing agent for PtO_2; however, this is proven incorrect as Pt can be captured from PtO_2 in a flow of synthetic air.[3,4] For Pt-catchment on Pd and Pd/Ni, Yang et al.[13] suggested that Pd works as a reducing agent for PtO_2, where Pd is oxidized to PdO and PtO_2 is reduced to Pt. This is suggested to occur because the affinity to oxygen is higher for Pd compared to Pt. However, in this study, we have observed that Au is actually a quite decent Pt-catchment material, capturing Pt at the same rate as Pd/Au (91/9 at. %) in laboratory experiments. This is supported by Holzmann,[5] where Au and Pd/Au (77/23 at. %) captured similar amounts of Pt. We suggest that the mechanism proposed by Yang et al.[13] is incorrect for Pt-catchment on Au as the oxides of Au have much lower stability than those of Pt.[40] The stability of PdO is also highly dependent on temperature and pO_2, and it is reported that PdO dominates the surface of a Pd/Pt alloy below 650 °C but not above .[41]

We now consider three key facts from this study:

1. For all samples in this study, the Pd/(Pd + Au) ratio is higher at Pt-rich locations, indicating that Pd has a higher affinity than Au toward Pt-catchment (Tables 2, 4). Oxygen alone does not cause the same attraction of Pd to the surface as during Pt-catchment (Figure S2; Table S1).

2. In the industrial experiment (Table 5), the obtained Pt concentration is higher for samples with a higher Pd content, while they are similar in the laboratory experiments (Table 1). Pd/Au (50/50 at. %) captures less Pt than Pd/Au (91/9 at. %) in the industrial experiments but equal quantities in the laboratory experiment.

3. The maximally measured Pt concentration (10−12 at. % in Au, >20 at. % in Pd) is much lower than the limitations of the phase diagram.[28,29]

This implies that the industrial gas mixture strongly affects the Pt-catchment abilities of the different Pd/Au samples, and the chemistry of species present (Pd, Au, Pt, O/O_2, NO, H_2O, NH_3, N_2O, NO_2) and gas-surface interactions participate in determining the Pt saturation concentration.

We question if PtO_2 is simply going through a decomposition into Pt metal and O_2 gas once it hits the metallic surface, but several factors affect this reaction. During Pt-catchment experiments, a black layer forms on the cold end of the quartz tubes, showing that PtO_2 will condense or decompose at some point.[42] PtO_2 (g) is simply generated by evaporation from a Pt surface due to heat and the presence of oxygen and may equally easily condense/decompose on a non-Pt-containing surface, if energetically favorable. This indicates that PtO_2 (g) is not a very stable species, and PtO_2 (g) may have an energetic gain by reacting from a gas-phase molecule to a solid Pt metal in an alloy material and simply release oxygen into the air. We believe the energetic gain of the reaction below can better describe the reactivity toward Pt-catchment

$$PtO_2(g) + Pd/Au(s) + E_{surface}^{Pd/Au} \rightarrow Pd/Au/Pt(s) + E_{surface}^{Pd/Au/Pt} + O_2(g)$$

There is likely a difference in gained energy for this reaction as a function of temperature, alloy composition (including Pt content), and gas mixture. The surface energy ($E_{surface}$) and possible surface segregation[41,43,44] and orientation[45] will likely be key factors; for example, surface segregation of Pd is expected in Pd/Au in NO gas at low temperature,[46] while the opposite is expected in vacuum.[43] The role of oxygen is also important as Pt-catchment is typically performed with pO_2 in the range of 0.05−0.7 bar (depending on total pressure). A higher pO_2 will cause a higher $pPtO_2$ and affect the oxidation state of the surface species. It has been demonstrated that a gas-surface equilibrium is likely the cause for the limiting Pt concentration that can be obtained from Pt-catchment,[39] and thus the surface activity of the different species is a key factor in this system, which again influences both the Pt-catchment rate and the rate of Pd and Au loss from the catchment material. We recommend that the Pt saturation concentration and variating Pd loss from the Pd/Au samples are further investigated for relevant gas mixtures and temperatures, ideally in connection with studies of surface segregation and surface species.

4.6. Future Development of Pd/Au Alloys for Pt-Catchment. The Pd/Au alloys have in this investigation proved to be a good alternative to the industrially used Pd/Ni (91/9 at. %) alloy. The degree of restructuring is low for Pd/Au (50/50 at. %), solving the major problem with the Pd/Ni gauze system. This fact makes it possible to install several gauzes in the gauze pack and ensure Pt-catchment over a large portion of the campaign. Further development could also be performed by testing ternary alloys and consider if additives in small quantities (X in Pd/Au/X) can aid the system, for example, by reducing grain growth and improving diffusional properties without causing grain reconstruction. X could be a non-noble metal that is oxidized during the initial use of the net and that plays its role as a binary oxide.

This investigation has also shown a low Pd and Au loss, even lower than that observed by Holzmann.[5] Holzmann found that the Pd loss was approximately one-third of the Pt-catchment in weight for several of the Pd/Au alloys. This implies that as long as the Pd/Au price is less than 3 times that of Pt, Pt-catchment using these alloys is beneficial. Further studies should address why the Pd loss is lower from the Pd/Au alloys compared to Pd and aim to reduce Pd loss further. Variations in the wire diameter could be tested, for example, thicker wires imply a lower surface area and could cause lower Pd/Au loss if the wire restructuring is not too severe. On the other hand, thinner wires could have higher Pt-catchment rates, which may be preferred. Variations in weave/knitting of the gauze (e.g., mesh size) should also be tested as it may improve the Pt-catchment abilities.

5. CONCLUSIONS

Laboratory Pt-catchment experiments using polycrystalline Pd/Au samples show that the three Pd/Au compositions [Pd/Au (91/9 at. %), Pd/Au (50/50 at. %), and Au] capture similar amounts of Pt, although less than Pd. The wire restructuring is reduced from Pd to Pd/Au (50/50 at. %), likely due to improved bulk diffusion relative to GB diffusion. The quasi-monocrystalline Pd/Au samples show a higher Pt concentration in the wire core with increasing Au content, demonstrating the improved

https://doi.org/10.1021/acs.iecr.2c02852
Ind. Eng. Chem. Res. 2023, 62, 2478−2493

bulk diffusion. The quasi-monocrystalline samples restructure very little; however, Au deviates from the trend and restructures both as poly- and quasi-monocrystalline wires. The restructuring of Au seems to proceed with a different mechanism than the Pd-containing samples.

In the industrial experiment, both the poly- and quasi-monocrystalline samples restructure in a similar manner in contrast to the laboratory experiments. Au reacts with the surrounding net during the industrial experiment and is therefore less suited for industrial applications. It is evident that the corrosion-like process causing wire restructuring is reduced due to the enhanced bulk diffusion of the Pd/Au (50/50 at. %) alloy. This implies that the Pd/Au (50/50 at. %) alloy or a similar composition (see the shaded area in Figure 11) has great potential as a new Pt-catchment material, with minimal grain reconstruction and a low Pd loss. Further pilot/industrial-scale testing should be performed to identify the optimal Pd/Au alloy.

■ ASSOCIATED CONTENT

Supporting Information

The Supporting Information is available free of charge at https://pubs.acs.org/doi/10.1021/acs.iecr.2c02852.

Additional SEM/EDX images of samples used and tested in the laboratory experiments; pictures of the samples before the industrial experiment; additional SEM/EDX images of the samples from the industrial experiment; additional quantitative EDX analysis of the industrial samples; results from diffusion model simulations using MATLAB; diffusion coefficients reported in the literature; and metal price of Pd and Pt from 2016 to 2022 (PDF)

■ AUTHOR INFORMATION

Corresponding Authors

Asbjørn Slagtern Fjellvåg − *Department of Chemistry, Centre for Materials Science and Nanotechnology, University of Oslo, N-0315 Oslo, Norway;* orcid.org/0000-0002-8587-5257; Email: a.s.fjellvag@smn.uio.no

Anja Olafsen Sjåstad − *Department of Chemistry, Centre for Materials Science and Nanotechnology, University of Oslo, N-0315 Oslo, Norway*; Email: a.o.sjastad@kjemi.uio.no

Authors

David Waller − *Yara Technology Center, 3936 Porsgrunn, Norway*

Thomas By − *K. A. Rasmussen, 2316 Hamar, Norway*

Complete contact information is available at: https://pubs.acs.org/10.1021/acs.iecr.2c02852

Notes

The authors declare no competing financial interest.

■ ACKNOWLEDGMENTS

The authors would like to thank Dr. Susmit Kumar (University of Oslo) for discussions on the topic of diffusion in metals and general discussions with the entire iCSI centre, the Catchment Team in iCSI, and the research group NAFUMA (University of Oslo). We would also like to acknowledge the expertise of Patrick Springer and MikroLab Kolbe in ICP−OES analysis. The project was financed by the Research Council of Norway through the project iCSI (project no. 237922).

■ REFERENCES

(1) Warner, M.The Kinetics of Industrial Ammonia Combustion. PhD Doctorate, The University of Sydney, 2013. Available from: http://hdl.handle.net/2123/9426.

(2) Hannevold, L.*Reconstruction of noble-metal catalysts during oxidation of ammonia*. PhD Doctorate, Department of Chemistry, University of Oslo, 2005.

(3) Fjellvåg, A. S.; Sjåstad, A. O.; Waller, D.; Skjelstad, J. Grain Reconstruction of Pd and Pd/Ni Alloys for Platinum Catchment. *Johnson Matthey Technol. Rev.* **2019**, *63*, 236.

(4) Fjellvåg, A. S.; Jørgensen, P. S.; Waller, D.; Wragg, D. S.; Michiel, M. D.; Sjåstad, A. O. Mechanism of grain reconstruction of Pd- and Pd/Ni wires during Pt-catchment. *Materialia* **2022**, *21*, 101359.

(5) Holzmann, H. Platin-Rückgewinnung bei der NH3-Verbrennung an Platin/Rhodium-Netzkatalysatoren. *Chem. Ing. Tech.* **1968**, *40*, 1229−1237.

(6) Pura, J.; Kwaśniak, P.; Jakubowska, D.; Jaroszewicz, J.; Zdunek, J.; Garbacz, H.; Mizera, J.; Gierej, M.; Laskowski, Z. Investigation of degradation mechanism of palladium-nickel wires during oxidation of ammonia. *Catal. Today* **2013**, *208*, 48−55.

(7) Ning, Y.; Yang, Z.; Zhao, H. Structure Reconstruction in Palladium Alloy Catchment Gauzes. *Platinum Met. Rev.* **1995**, *39*, 19−26.

(8) Fierro, J.; Palacios, J.; Tomas, F. Characterization of catalyst and catchment gauzes used in medium- and low-pressure ammonia oxidation plants. *J. Mater. Sci.* **1992**, *27*, 685−691.

(9) Fierro, J. L. G.; Palacios, J. M.; Tomás, F. Redistribution of Platinum Metals within an Ammonia Oxidation Plant. *Platinum Met. Rev.* **1990**, *34*, 62−70.

(10) Fierro, J. L. G.; Palacios, J. M.; Tomás, F. Morphological and chemical changes in palladium alloy gauzes used for platinum recovery in high-pressure ammonia oxidation plants. *Surf. Interface Anal.* **1989**, *14*, 529−536.

(11) Ning, Y.; Yang, Z. Platinum loss from alloy catalyst gauzes in nitric acid plants: The important role of the palladium component in metal capture during ammonia oxidation. *Platinum Met. Rev.* **1999**, *43*, 62−69.

(12) Ning, Y.; Yang, Z.; Zhao, H. Platinum recovery by palladium alloy catchment gauzes in nitric acid plants: The mechanism of platinum recovery. *Platinum Met. Rev.* **1996**, *40*, 80−87.

(13) Yang, Z.; Ning, Y.; Zhao, H. Changes of composition and surface state of palladium-nickel alloy gauzes used in ammonia oxidation apparatus. *J. Alloys Compd.* **1995**, *218*, 51−57.

(14) Pura, J.; Wieciński, P.; Kwaśniak, P.; Zwolińska, M.; Garbacz, H.; Zdunek, J.; Laskowski, Z.; Gierej, M. Investigation of the degradation mechanism of catalytic wires during oxidation of ammonia process. *Appl. Surf. Sci.* **2016**, *388*, 670−677.

(15) Pura, J.; Garbacz, H.; Zdunek, J.; Mizera, J.; Gierej, M.; Laskowski, Z. Analysis of two catalytic systems PtRhPd-PdAu and PtRh-PdAu after long-term exploitation. *Inżynieria Materiałowowa* **2013**, *4*, 358−362.

(16) Heywood, A. E. The Recovery of Platinum from Ammonia Oxidation Catalysts. *Platinum Met. Rev.* **1982**, *26*, 28−32.

(17) Heywood, A. E. Platinum Recovery in Ammonia Oxidation Plants. *Platinum Met. Rev.* **1973**, *17*, 118−129.

(18) Han, F.; Liu, X. Comparison of Pt catchment between two Pd alloy in nitric acid catalyst gauze. *Guijinshu* **2017**, *38*, 31−35.

(19) Haugsrud, R. On the high-temperature oxidation of nickel. *Corros. Sci.* **2003**, *45*, 211−235.

(20) Young, D. J.*High Temperature Oxidation and Corrosion of Metals*; Corrosion Series; Elsevier Science & Technology: Jordan Hill, 2008; Vol. *1*. ISBN: 978008044587800804458 7X.

(21) Kim, C. U. In *Electromigration in thin films and electronic devices : materials and reliability*; Kim, C.-U., Ed.; Woodhead Publishing: Oxford Philadelphia, 2011.

(22) Kim, D.; Chang, J.-h.; Park, J.; Pak, J. J. Formation and behavior of Kirkendall voids within intermetallic layers of solder joints. *J. Mater. Sci.: Mater. Electron.* **2011**, *22*, 703−716.

(23) Zacharaki, E.; Beato, P.; Tiruvalam, R. R.; Andersson, K. J.; Fjellvåg, H.; Sjåstad, A. O. From Colloidal Monodisperse Nickel Nanoparticles to Well-Defined Ni/Al_2O_3 Model Catalysts. *Langmuir* **2017**, *33*, 9836−9843.
(24) Klinger, L.; Rabkin, E. Theory of the Kirkendall effect during grain boundary interdiffusion. *Acta Mater.* **2011**, *59*, 1389−1399.
(25) Rabkin, E.; Klinger, L.; Izyumova, T.; Semenov, V. N. Diffusion-induced grain boundary porosity in NiAl. *Scr. Mater.* **2000**, *42*, 1031−1037.
(26) Chee, S. W.; Wong, Z. M.; Baraissov, Z.; Tan, S. F.; Tan, T. L.; Mirsaidov, U. Interface-mediated Kirkendall effect and nanoscale void migration in bimetallic nanoparticles during interdiffusion. *Nat. Commun.* **2019**, *10*, 2831.
(27) Baheti, V. A.; Ravi, R.; Paul, A. Interdiffusion study in the Pd-Pt system. *J. Mater. Sci.: Mater. Electron.* **2013**, *24*, 2833−2838.
(28) Smithells, C. J.Smithells metals reference book = Metals reference book. In *Metals Reference Book*; Totemeier, T. C., Gale, W. F., Eds.; Elsevier Butterworth-Heinemann: Amsterdam Boston, 2004.
(29) Neumann, G. In *Self-Diffusion and Impurity Diffusion in Pure Metals: Handbook of Experimental Data*; Tuijn, C., Ed.; Pergamon: Amsterdam, Boston, London, 2009.
(30) Okamoto, H.; Massalski, T. B. The Au−Pd (Gold-Palladium) system. *Bull. Alloy Phase Diagrams* **1985**, *6*, 229−235.
(31) Debonte, W. J.; Poate, J. M. Low temperature interdiffusion in the Au-Pd and Au-Rh thin film couples. *Thin Solid Films* **1975**, *25*, 441−448.
(32) Murakami, M.; deFontaine, D.; Fodor, J. X-ray diffraction study of interdiffusion in bimetallic Au/Pd thin films. *J. Appl. Phys.* **1976**, *47*, 2850−2856.
(33) Raub, E.; Wörwag, G. Die Gold-Platin-Palladium-Legierungen. *Z. Metallkd.* **1955**, *46*, 513−515.
(34) Kubaschewski, O.; Counsell, J. F. Thermodynamische Eigenschaften des Systems Gold-Platin-Palladium. *Monatsh. Chem.* **1971**, *102*, 1724−1728.
(35) Neukam, O. Diffusionsüberzüge. *Galvanotechnik (Saulgau/Württ.)* **1970**, *61*, No. 8.
(36) The MathWorks Inc.*MATLAB*, 2019. [9.7.0.1247435 (2019b)].
(37) Opila, E. J.University of Virginia. Unpublished work.
(38) Cho, J. H.; Kim, Y. W.; Oh, K. H.; Cho, J. S.; Moon, J. T.; Lee, J.; Cho, Y. W.; Rollett, A. D. Recrystallization and grain growth of cold-drawn gold bonding wire. *Metall. Mater. Trans. A* **2003**, *34*, 1113−1125.
(39) Håkonsen, S. F.; Holme, B.; Waller, D.An investigation of the limiting factors for Pt catchment in the Ostwald process. To be published, **2022**.
(40) Hämäläinen, J.; Ritala, M.; Leskelä, M. Atomic Layer Deposition of Noble Metals and Their Oxides. *Chem. Mater.* **2014**, *26*, 786−801.
(41) Li, T.; Bagot, P. A. J.; Marquis, E. A.; Edman Tsang, S. C.; Smith, G. D. W. Atomic engineering of platinum alloy surfaces. *Ultramicroscopy* **2013**, *132*, 205−211.
(42) Knoops, H. C.; Mackus, A.; Donders, M.; Van de Sanden, M. C.; Notten, P.; Kessels, W. M. Remote Plasma and Thermal ALD of Platinum and Platinum Oxide Films. *ECS Trans.* **2008**, *16*, 209−218.
(43) Ruban, A. V.; Skriver, H. L.; Nørskov, J. K. Surface segregation energies in transition-metal alloys. *Phys. Rev. B: Condens. Matter Mater. Phys.* **1999**, *59*, 15990−16000.
(44) Li, T.; Marquis, E. A.; Bagot, P. A. J.; Tsang, S. C.; Smith, G. D. W. Characterization of oxidation and reduction of a platinum−rhodium alloy by atom-probe tomography. *Catal. Today* **2011**, *175*, 552−557.
(45) Bagot, P. A. J.; Cerezo, A.; Smith, G. D. W. 3D atom probe study of gaseous adsorption on alloy catalyst surfaces III: Ternary alloys − NO on Pt−Rh−Ru and Pt−Rh−Ir. *Surf. Sci.* **2008**, *602*, 1381−1391.
(46) de Bocarmé, T. V.; Moors, M.; Kruse, N.; Atanasov, I. S.; Hou, M.; Cerezo, A.; Smith, G. D. W. Surface segregation of Au-Pd alloys in UHV and reactive environments: quantification by a catalytic atom probe. *Ultramicroscopy* **2009**, *109*, 619.

https://doi.org/10.1021/acs.iecr.2c02852
Ind. Eng. Chem. Res. 2023, 62, 2478−2493